

See discussions, stats, and author profiles for this publication at: <https://www.researchgate.net/publication/233817717>

# 3D-QSAR and docking studies of benzoyl urea derivatives as tubulin-binding agents for antiproliferative activity

ARTICLE *in* MEDICINAL CHEMISTRY RESEARCH · MARCH 2013

Impact Factor: 1.4 · DOI: 10.1007/s00044-012-0139-2

---

CITATION

1

---

READS

75

## 2 AUTHORS:



[Deepak Lokwani](#)

Dr. Babasaheb Ambedkar Marathwada Uni...

19 PUBLICATIONS 100 CITATIONS

SEE PROFILE



[Devanand Shinde](#)

Dr. Babasaheb Ambedkar Marathwada Uni...

279 PUBLICATIONS 1,606 CITATIONS

SEE PROFILE

# *3D-QSAR and docking studies of benzoyl urea derivatives as tubulin-binding agents for antiproliferative activity*

**Deepak K. Lokwani, Aniket P. Sarkate & Devanand B. Shinde**

## **Medicinal Chemistry Research**

ISSN 1054-2523

Volume 22

Number 3

Med Chem Res (2013) 22:1415-1425

DOI 10.1007/s00044-012-0139-2



**Your article is protected by copyright and all rights are held exclusively by Springer Science+Business Media, LLC. This e-offprint is for personal use only and shall not be self-archived in electronic repositories. If you wish to self-archive your work, please use the accepted author's version for posting to your own website or your institution's repository. You may further deposit the accepted author's version on a funder's repository at a funder's request, provided it is not made publicly available until 12 months after publication.**

## 3D-QSAR and docking studies of benzoyl urea derivatives as tubulin-binding agents for antiproliferative activity

Deepak K. Lokwani · Aniket P. Sarkate ·  
Devanand B. Shinde

Received: 28 November 2011 / Accepted: 31 May 2012 / Published online: 17 June 2012  
© Springer Science+Business Media, LLC 2012

**Abstract** Tubulins, an  $\alpha\beta$  heterodimers, the major component of microtubules, are important molecular target of numerous small molecule ligands for anticancer therapy. In this study, the molecular modeling studies were performed to develop predictive 3D-QSAR models using set of 32 compounds of benzoyl urea derivatives as tubulin-binding agents for antiproliferative activity. A five-point common pharmacophore hypotheses with one hydrogen bond acceptor (A), two hydrogen bond donors (D), one hydrophobic (H), and one ring (R) vector features were selected for alignment of all compounds. The 3D-QSAR models generated using training set of 21 compounds and test set of 11 compounds showed good partial least squares statistical results. The developed CPHs and 3D-QSAR models were validated further externally by predicting the activity of database of compounds from literature and comparing it with actual activity. Docking studies were also carried out for all compounds on colchicine-binding site of  $\beta$ -tubulin for studying of binding affinity of compounds for antiproliferative activity. The results of these molecular modeling studies are helpful to refine the pharmacophore for design of new potential compounds for antiproliferative activity.

**Keywords** 3D-QSAR ·  $\beta$ -Tubulin · Antiproliferative activity · Benzoyl urea · Docking

### Introduction

Microtubules (MTs), major structural components in cells, are the target of a large and diverse group of natural product anticancer drugs (Jordan and Wilson, 2004). MTs are polymeric protein complexes constructed from a heterodimer of two highly homologous proteins known as  $\alpha$ - and  $\beta$ -tubulin. The assembly of tubulin heterodimers into a macromolecular MT complex is a tightly regulated and dynamic process. MTs have essential roles in vital cellular functions, such as motility, division, shape maintenance, and intracellular transport (Verhey and Gaertig, 2007; Pellegrini and Budman, 2005). Tubulin is therefore target of numerous small molecule ligands that interfere with MT dynamics, several of which are of clinical use, in particular for cancer treatment (Kiselyov *et al.*, 2007; Jeffrey *et al.*, 2007; Giannakakou *et al.*, 2000). A structurally diverse collection of ligands, such as vinblastine sulfate, colchicine, combretastatin A-4 (Pettit *et al.*, 1989), the epothilones (Goodin *et al.*, 2004) and paclitaxel (Wani *et al.*, 1971; Schiff and Horwitz, 1980) as well as some synthetic molecules (Yoshimatsu *et al.*, 1997; Arora *et al.*, 2009) are known to exert cytotoxic activities through binding to tubulin. Recently, much effort has been devoted to the identification of new compounds from both natural and synthetic sources that bind at the colchicine site of tubulin (Li and Sham, 2002; Kingston, 2009; Beckers and Mahboobi, 2003). Mutations in  $\beta$ -tubulin that affect MT polymer mass and/or drug binding are associated with resistance to tubulin-binding agents such as paclitaxel (Kavallaris, 2010). Also, independent of the precise mechanism of action, clinical use of antitubulin drugs is associated with problems of drug toxicity and bioavailability (Sridhare *et al.*, 2004). Therefore, there is a need to find new tubulin-binding agents for anticancer activity.

**Electronic supplementary material** The online version of this article (doi:10.1007/s00044-012-0139-2) contains supplementary material, which is available to authorized users.

D. K. Lokwani · A. P. Sarkate · D. B. Shinde (✉)  
Department of Chemical Technology, Dr. Babasaheb Ambedkar  
Marathwada University, Aurangabad 431004 (MS), India  
e-mail: dbsdeepak10@rediffmail.com

Recently, the benzoyl urea analogs have shown good anticancer activity and become new family of tubulin-binding agents (Song *et al.*, 2008; Ling *et al.*, 2002; Ling *et al.*, 2003; Jiang *et al.*, 2002; Li *et al.*, 2003; Hwang *et al.*, 2002).

We have previously demonstrated the use of energetic pharmacophore for the designing of cyclooxygenase-2 inhibitors (Lokwani *et al.*, 2012) and used docking study for predicting the binding affinity of targets such as non-nucleoside reverse transcriptase inhibitors (Mokale *et al.*, 2012). In search of new targets using computational studies, we present here the correlation of structures of benzoyl urea analogs with antiproliferative activity. Thus, to optimize this pharmacophore and for further improving the activity, we developed atom-based 3D-QSAR models using pharmacophore alignment and scoring engine (PHASE) and performed docking study on colchicine-binding site of  $\beta$ -tubulin using grid-based ligand docking with energetics (GLIDE). PHASE is self contained system for pharmacophore perception, QSAR model development, and 3D database screening (Dixon *et al.*, 2006). We validated developed 3D-QSAR models internally by predicting the activity of test set and externally by predicting the activity of compounds obtained from literature. The GLIDE docking module approximated a complete systematic search of the conformational, orientational, and positional space of the docked ligand molecules into the receptor-binding pocket (Friesner *et al.*, 2004). The developed atom-based 3D-QSAR model and docking studies highlight the structural features of benzoyl urea analogs for binding to colchicine-binding site of  $\beta$ -tubulin which is useful for further design of more potent tubulin-binding agent having antiproliferative activity.

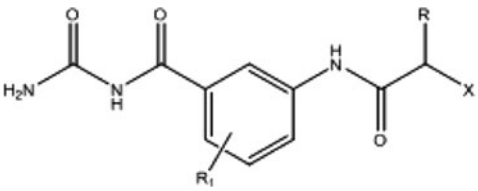
## Materials and methods

### Biological data

A set of 32 benzoyl urea analogs (Table 1) with available  $IC_{50}$  data for antiproliferative activity were taken from literature (Song *et al.*, 2008) for the development of ligand-based CPHs. The negative logarithm of the measured  $IC_{50}$  value ( $pIC_{50}$ ) was used in this study. For 3D-QSAR studies, these 32 compounds were divided into a training set (21 compounds) and a test set (11 compounds). The training set molecules were selected randomly in such a way that they contained information in terms of both their structural features and biological activity ranges. The most active molecules, moderately active, and less active molecules were included in training set to spread out the range of activities. In order to assess the predictive power of the

model, a set of 11 compounds was arbitrarily set aside as the test set. The test compounds were selected in such a way that they truly represent the training set.

**Table 1** Structure of compounds used for development of common pharmacophore hypothesis and 3D-QSAR studies along with biological activity



S. no.	Compounds	R <sub>1</sub>	X	R	Biological activity	
					IC <sub>50</sub>	pIC <sub>50</sub>
1	<b>1</b>	H	Br	CH <sub>3</sub>	1.47	−0.167
2	<b>10c<sup>a</sup></b>	2-CH <sub>3</sub>	Br	CH <sub>3</sub>	0.48	0.319
3	<b>10d</b>	4-CH <sub>3</sub>	Br	CH <sub>3</sub>	3.36	−0.526
4	<b>10f<sup>a</sup></b>	4-F	Br	CH <sub>3</sub>	3.13	−0.496
5	<b>10g</b>	6-F	Br	CH <sub>3</sub>	0.52	0.284
6	<b>10h</b>	4-Cl	Br	CH <sub>3</sub>	9.80	−0.991
7	<b>10i</b>	6-Cl	Br	CH <sub>3</sub>	2.55	−0.406
8	<b>10j</b>	6-Br	Br	CH <sub>3</sub>	7.63	−0.882
9	<b>10l<sup>a</sup></b>	5-COOCH <sub>3</sub>	Br	CH <sub>3</sub>	2.7	−0.431
10	<b>10m<sup>a</sup></b>	5-NO <sub>2</sub>	Br	CH <sub>3</sub>	1.58	−0.199
11	<b>2<sup>a</sup></b>	H	Br	H	0.725	0.143
12	<b>11a</b>	2-CH <sub>3</sub>	Br	H	1.71	−0.233
13	<b>11b</b>	4-CH <sub>3</sub>	Br	H	4.28	−0.631
14	<b>11c<sup>a</sup></b>	6-CH <sub>3</sub>	Br	H	4.76	−0.678
15	<b>11d</b>	4-F	Br	H	2.29	−0.36
16	<b>11e</b>	6-F	Br	H	0.01	2
17	<b>11f</b>	4-Cl	Br	H	2.91	−0.464
18	<b>11g</b>	6-Cl	Br	H	0.54	0.268
19	<b>11h</b>	6-Br	Br	H	1.16	−0.064
20	<b>11i<sup>a</sup></b>	4-OCH <sub>3</sub>	Br	H	1.88	−0.274
21	<b>11j</b>	5-COOCH <sub>3</sub>	Br	H	1.3	−0.114
22	<b>11k<sup>a</sup></b>	5-NO <sub>2</sub>	Br	H	1.53	−0.185
23	<b>11l</b>	6-OCH <sub>3</sub>	Br	H	1.57	−0.196
24	<b>13a</b>	2-CH <sub>3</sub>	Cl	H	2.70	−0.431
25	<b>13b</b>	4-CH <sub>3</sub>	Cl	H	3.36	−0.526
26	<b>13d</b>	6-F	Cl	H	7.68	−0.885
27	<b>13e<sup>a</sup></b>	4-Cl	Cl	H	15.9	−1.201
28	<b>13f<sup>a</sup></b>	6-Cl	Cl	H	2.44	−0.387
29	<b>3<sup>a</sup></b>	H	I	H	0.01	2
30	<b>14a</b>	6-CH <sub>3</sub>	I	H	20.0	−1.301
31	<b>14b</b>	6-F	I	H	0.01	2
32	<b>14c</b>	5-COOCH <sub>3</sub>	I	H	1.91	−0.281

<sup>a</sup> Compounds in test set

## Ligand preparation

The structure of each compounds were cleaned and optimized using Ligprep v2.4 (Schrödinger, LLC, New York, NY, 2009). The cleanup and optimization process include conversion of structures from 2D to 3D, addition of hydrogen atoms, removal of counter ions, ionization state at the pH 7.0, generation of stereoisomers, removal of noncompliant structures, and energy minimization. Conformers of all ligands were generated using ConfGen macromodel search method (Watts *et al.*, 2010) with maximum number of conformers 1,000 per structure and minimization steps 100 and minimized using OPLS\_2005 force field (Jorgensen *et al.*, 1996). Each minimized conformer was further filtered to eliminate redundant conformations. For each molecule, a set of conformers with maximum energy difference of 10 kcal/mol relative to global energy minimum conformers were retained. Also, conformers with the RMSD of lower than 1.0 Å between all pairs of corresponding heavy atoms were considered identical and discarded.

## Generation of the common pharmacophore hypotheses (CPHs)

Pharmacophore features; hydrogen bond acceptor (A), hydrogen bond donor (D), hydrophobic group (H), negatively charged group (N), positively charged group (P), and aromatic ring (R) were defined by a set of chemical structure patterns as SMARTS queries. Common pharmacophoric features were then identified from a set of variants (set of feature types) that define a possible pharmacophore using a tree-based partitioning algorithm with maximum tree depth of four with the requirement that all actives must match. After applying default feature definitions to each ligand, CPHs were generated using a final box of 1 Å.

All generated CPHs were examined and selected based on a scoring function to yield the best alignment of the active ligands using an overall maximum root mean square deviation (RMSD) value of 1.2 Å with default options for distance tolerance. The quality of alignment was measured by a survival score, defined as

$$S = W_{\text{site}} S_{\text{site}} + W_{\text{vec}} S_{\text{vec}} + W_{\text{vol}} S_{\text{vol}} + W_{\text{sel}} S_{\text{sel}} + W_{\text{rev}}^m - W_E \Delta E + W_{\text{act}} A$$

where  $W$  is the weight and the  $S$  is the score;  $S_{\text{site}}$  is based on alignment score which is RMSD in the site point position as

$$S_{\text{site}}(i) = 1 - S_{\text{align}}(i)/C_{\text{align}}(i)$$

$S_{\text{align}}(i)$  represents alignment score and  $C_{\text{align}}(i)$  is RMSD cutoff (default value 1.2 Å);  $S_{\text{vec}}$  represents vector score which is average cosine of the angles formed by

corresponding pairs of vector features (acceptor, donors, and aromatic rings) in aligned structures;  $S_{\text{vol}}$  represents volume score based on overlap of van der Waals model of non-hydrogen atoms in each pair of structures

$$S_{\text{vol}}(i) = V_{\text{common}}(i)/V_{\text{total}}(i)$$

where  $V_{\text{common}}(i)$  is common or overlapping volume between ligand  $i$  and the reference ligand, while  $V_{\text{total}}(i)$  is the total volume occupied by both ligand;  $S_{\text{sel}}$  is the selectivity score which is an empirical estimate of the rarity of hypothesis, and accounts for what fraction of molecules are likely to match the hypothesis regardless of their activity toward the receptor;  $W_{\text{rev}}^m$  is the reward weights defined by  $m - 1$ , where  $m$  is the number of actives that match the hypothesis;  $\Delta E$  is a penalty for high energy structures by subtracting a multiple of the relative energy from final score;  $A$  is the penalty for hypotheses for which the reference ligand activity is lower than the highest activity, by adding a multiple of the reference ligand activity to the score;  $W_{\text{site}}$ ,  $W_{\text{vec}}$ ,  $W_{\text{vol}}$ ,  $W_{\text{rev}}$ , and  $W_{\text{act}}$ , have default values of 1.0, while  $W_{\text{sel}}$  and  $W_E$  has a default value of 0.0. In hypothesis generation, default values have been used.

The CPHs with high survival score were chosen for alignment of molecules and used for further 3D-QSAR studies.

## Building of 3D-QSAR models

Atom-based 3D-QSAR models were developed using partial least squares (PLS) regression analysis for the top four CPHs based on their survival score. In atom-based 3D-QSAR in PHASE, each molecule is treated as a set of overlapping van der Waals spheres. Each atom (and hence each sphere) is placed into one of six categories according to a simple set of rules: hydrogens attached to polar atoms are classified as hydrogen bond donors (D); carbons, halogens, and C–H hydrogens are classified as hydrophobic/non-polar (H); atoms with an explicit negative ionic charge are classified as negative ionic (N); atoms with an explicit positive ionic charge are classified as positive ionic (P); non-ionic atoms are classified as electron withdrawing (W); and all other types of atoms are classified as miscellaneous (X). For construction of atom-based 3D-QSAR model, a rectangular grid of cubes (1 Å on each side) were defined for aligned training set for occupation of all atoms. Each occupied cubes were allotted one or more volume bits to represent the molecules by string of zero and ones. This representation gives rise to binary-valued occupation patterns that was used as independent variables to create PLS QSAR models (Dixon *et al.*, 2006). The PLS regression was carried out with maximum of  $N/5$  PLS factors, where  $N$  is the number of ligands in training set.



## Docking method

The molecular docking tool, Glide v5.6 (Schrödinger, LLC, New York, NY, 2009) was used for docking studies of all compounds on colchicine-binding site of  $\beta$ -tubulin. The crystal structure of  $\beta$ -tubulin was obtained from protein data bank (PDB code: 1SA0) and was prepared for docking using “protein preparation wizard” in Maestro wizard v9.1 (Schrödinger, LLC, New York, NY, 2009). Water molecules in the crystal structures were deleted and termini were capped by adding ACE and NMA residue. The protein preparation was carried out in two steps, preparation and refinement. In preparation component, after ensuring chemical correctness, the hydrogens were added where hydrogen atoms were missing. Side chains that are not close to the binding cavity and do not participate in salt bridges were neutralized. In the refinement component, a restrained impact minimization of the co-crystallized complex was carried out. This helps in reorientation of side chain hydroxyl group. It uses the OPLS\_2005 force field for this purpose. Grids were defined by centering them on the ligand in the crystal structure using the default box size.

The ligands were built using maestro build panel and prepared by Ligprep v2.4 (Schrödinger, LLC, New York, NY, 2009) which produces the low energy conformer of ligands using OPLS\_2005 force field. The lower energy conformations of the ligands were selected and were docked into the grid generated from protein structures using standard precision (SP) docking mode.

## Results and discussion

### Generation of 3D-QSAR models

Different variant CPHs were generated by common pharmacophore identification process. All CPHs were examined and scored to identify the pharmacophore that yields the best alignment of the active compounds ( $\text{pIC}_{50} > 0.0$ ). All CPHs were validated by aligning and scoring the inactive compounds ( $\text{pIC}_{50} < -0.3$ ). We have selected top four CPHs models whose survival-inactive scores ranked in

the top 1 % for alignment of all compounds and 3D-QSAR studies. The survival score for these CPHs is shown in Table 2. All top four CPHs were found to be associated with the five-point hypotheses, which consists of one hydrogen bond acceptor (A), two hydrogen bond donors (D), one hydrophobic (H), and one aromatic ring (R) vector features. All compounds were aligned using CPH ADDHR.102 for 3D-QSAR study (Fig. 1).

All top CPHs were used for atom-based 3D-QSAR model generation. The CPH ADDHR.102 yielded a 3D-QSAR model with good value of regression coefficient, low standard deviation, and high variance ratio with good stability, but showed diminished predictive power along with high RMSE value and low Pearson  $R$  value which stand for correlation between predicted and observed activity for test set. Similarly, CPH ADDHR.232 yielded a 3D-QSAR model with good statistical values but showed low predictive power ( $Q^2 = 0.4927$ ) (Table 3). The CPHs ADDHR.11 and ADDHR.245 yielded 3D-QSAR models with good PLS statistical values. Both these hypotheses showed good internal as well as external predictive power. The training set correlation in both CPHs is characterized by PLS factors ( $R^2 = 0.7217$ ,  $\text{SD} = 0.4705$ ,  $F = 14.7$ ,  $P = 5.641\text{e}-005$ ,  $Q^2 = 0.5982$  for CPH ADDHR.11 and  $R^2 = 0.7282$ ,  $\text{SD} = 0.4651$ ,  $F = 15.2$ ,  $P = 4.641\text{e}-005$ ,  $Q^2 = 0.5297$  for CPH ADDHR.245). The test set correlation is characterized by PLS factors (RMSE = 0.5304, Pearson  $R = 0.7962$  for CPH ADDHR.11 and RMSE = 0.4902, Pearson  $R = 0.769$  for CPH ADDHR.245).

We have selected the 3D-QSAR models generated by CPHs ADDHR.11 and ADDHR.245 for correlating the structure with activity. Graph of observed versus predicted biological activity of training and test sets are shown in Figs. 2 and 3, respectively. Residuals values obtained by subtraction of predicted activities from observed biological activities are near to zero which indicated that error in prediction of biological activity is low and predicting ability of QSAR models developed by CPHs ADDHR.11 and ADDHR.245 is good (Table 4). Mean of residual in predicting the activity of compounds was calculated by average of summation of all residual values. 3D-QSAR models associated with hypotheses ADDHR.11 and ADDHR.245 showed 0.3659 and 0.3167, respectively, as

**Table 2** Survival score of top four CPHs

S. no.	CPHs	Survival	Site	Vector	Volume	Inactive	Survival-inactive
1	ADDHR.102	8.409	0.84	0.995	0.8	2.505	5.904
2	ADDHR.11	8.402	0.86	0.959	0.814	2.468	5.934
3	ADDHR.245	8.394	0.84	0.994	0.791	2.496	5.898
4	ADDHR.232	8.394	0.85	0.992	0.785	2.505	5.889

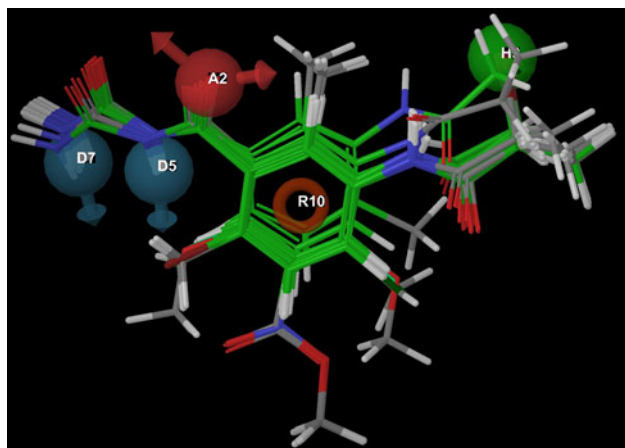


**Fig. 1** Alignment of all compounds using CPH ADDHR.102

the mean of residual which also support the predictability of both QSAR models. The pharmacophore hypothesis showing distance between pharmacophoric sites is depicted in Fig. 4.

Both 3D-QSAR models developed using CPHs ADDHR.11 and ADDHR.245 were applied to database of compounds taken from literature (Song *et al.*, 2008, 2009a, b; Hu *et al.*, 2007) for validation purpose. The activity of these reported compounds having benzoyl urea or similar pharmacophoric group were predicted and compared with its actual activity (Supplementary Data). The residual values obtained by subtraction of predicted activity from reported activity was found to be near zero for number of compounds. The mean of residual was also calculated and found as 0.529 and 0.484 for 3D-QSAR models associated with CPHs ADDHR.11 and ADDHR.245, respectively. These results suggested that correctness and capability of 3D-QSAR models developed by CPHs ADDHR.11 and ADDHR.245 for prediction of activity of compounds which can be applied to newly designed compounds for the prediction of their activity prior to synthesis.

Based on overall statistical results, 3D-QSAR model developed using CPHs ADDHR.11 were applied to each

compound in the series for the establishment of structure–activity correlation. A pictorial representation of the cubes generated in the present 3D-QSAR is shown in Figs. 5 and 6. In these generated cubes, the blue cubes indicate favorable features, while red cubes indicate unfavorable features for biological activity. The blue cubes around the hydrogen bond acceptor and hydrogen bond donor group of benzoyl urea suggest the importance of core ring for activity.

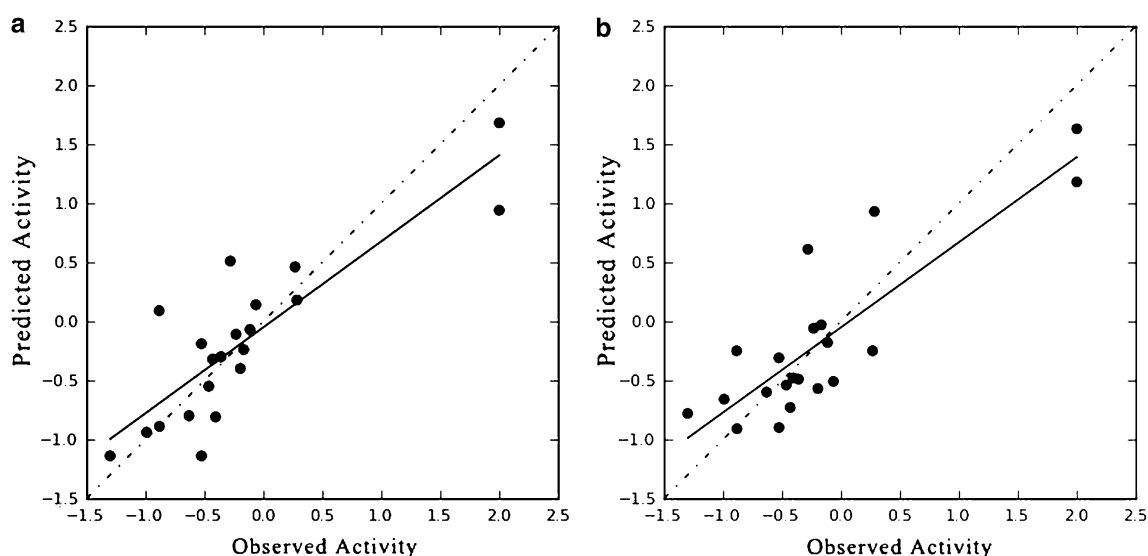
The substitutions around aromatic ring were observed to have small hydrophobic group and electron withdrawing group alone or both. The comparison of the most significant favorable and unfavorable interactions were observed when the 3D-QSAR model was visualized in the context of most active ligand (compound **31**) and the least active ligand (compound **30**) (Fig. 5). The blue cubes were observed at the position C<sub>6</sub> at phenyl ring near hydrogen bond acceptor (A2) vector which indicated that for better activity the ring should be substituted with halogen atom (Fig. 5a). Thus, compounds having substituted ring at position C<sub>6</sub> with halogen atom (compounds **7**, **16**, **18**, **19**, **31**) are more active than compounds having substituted ring with other groups (compounds **14**, **30**). Moreover, Figs. 5 and 6 showed the importance of fluorine atom for activity among the all halogen atom as hydrophobic group. However, some compounds containing fluorine atom at the position C<sub>6</sub> at phenyl ring were shown the moderate or lower activity, but this may be due to the replacement of hydrophobic group (H9) –Br or –I by –Cl near to Hydrogen bond acceptor (A1). This is proved in Fig. 6b, where blue cubes were observed around fluorine atom at the position C<sub>6</sub> and red cubes around hydrophobic group (H9) –Cl near to hydrogen bond acceptor (A1) in compound **26**.

Figure 6 shows features at position C<sub>4</sub> and C<sub>5</sub> which indicated that for better activity ring should un-substituted at these position. Therefore, compounds substituted by –Cl, CH<sub>3</sub>, and OCH<sub>3</sub> groups at position C<sub>4</sub> and –COOCH<sub>3</sub> or NO<sub>2</sub> group at position C<sub>5</sub> showed lower and moderate activity, respectively. This also indicated that substitution

**Table 3** Statistical results of 3D-QSAR model developed using different CPHs

S. no.	Statistic parameters	3D-QSAR models			
		ADDHR.102	ADDHR.232	ADDHR.11	ADDHR.245
1	SD	0.3605	0.4086	0.4705	0.4651
2	$R^2$	0.8366	0.7902	0.7217	0.7282
3	$F$	29	21.3	14.7	15.2
4	$P$	6.502e–007	5.326e–006	5.641e–005	4.641e–005
5	Stability	0.5922	0.3921	0.2599	0.5756
6	RMSE	0.69	0.5508	0.4902	0.5304
7	$Q^2$	0.204	0.4927	0.5982	0.5297
8	Pearson $R$	0.4742	0.7362	0.7962	0.769





**Fig. 2** Plot of observed activity versus predicted activity for training set for 3D-QSAR model generated using CPHs: **a** ADDHR.11, **b** ADDHR.245

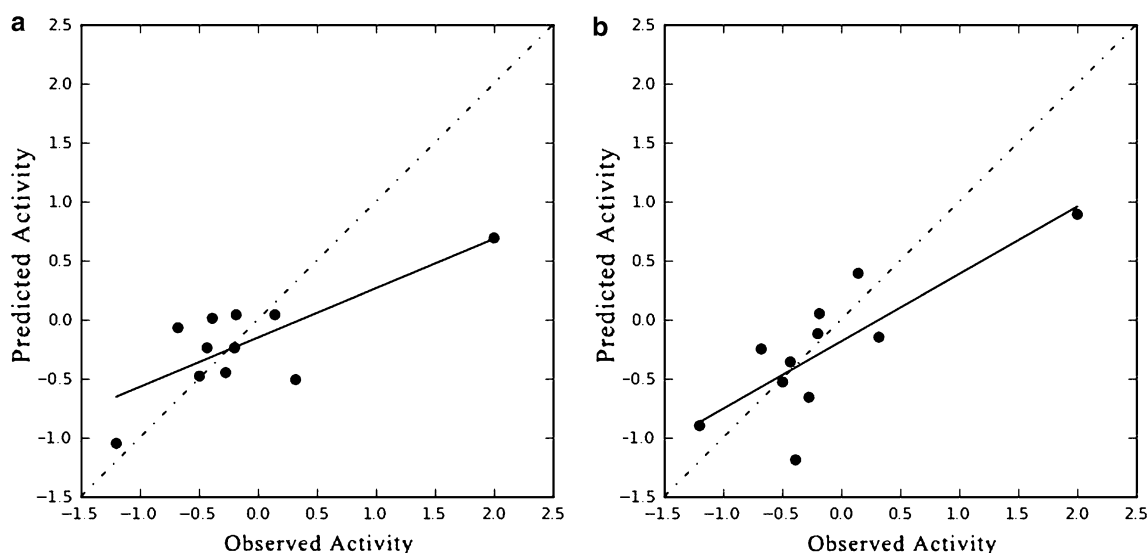


**Fig. 3** Plot of observed activity versus predicted activity for test set for 3D-QSAR model generated using CPHs: **a** ADDHR.11, **b** ADDHR.245

by electron withdrawing groups alone or along with hydrophobic groups lower down the activity.

#### Docking studies

All structures were docked to colchicine-binding site of  $\beta$ -tubulin for studying of binding mode of compounds for antiproliferative activity. The constraint was defined as reported in literature that all compounds should bind to SH group of CYS 241 by hydrogen bond. The reliability of the docking results was first checked by comparing the best

docking poses obtained for the co-crystallized inhibitor with its bound conformation. This was done by removing colchicine from their active site and subjecting again to docking into the binding pocket in the conformation found in the crystal structure. As a result, a RMSD of 1.36 and 0.25 Å were found for rigid and flexible docking which suggested that the docking procedure could be relied on to predict the binding mode of our compounds.

It was observed from docking results that all benzoyl urea analogs have a similar binding mode like colchicines in the binding pockets of  $\beta$ -tubulin (Fig. 7). The amino

**Table 4** Comparison of observed biological activity and predicted activity along with fitness of compounds on CPHs

S. no.	Compounds	Observed activity	3D-QSAR models					
			ADDHR.11			ADDHR.245		
			Predicted activity	Residual	Fitness	Predicted activity	Residual	Fitness
1	<b>11e</b>	2	1.18	0.82	3	0.94	1.06	3
2	<b>3<sup>a</sup></b>	2	0.89	1.11	2.62	0.69	1.31	2.61
3	<b>14b</b>	2	1.63	0.37	2.71	1.68	0.32	2.67
4	<b>10c<sup>a</sup></b>	0.319	−0.15	0.469	1.82	−0.51	0.829	2.29
5	<b>10g</b>	0.284	0.93	−0.646	2.88	0.18	0.104	2.46
6	<b>11g</b>	0.268	−0.25	0.518	2.87	0.46	−0.192	2.85
7	<b>2<sup>a</sup></b>	0.143	0.39	−0.247	2.88	0.04	0.103	2.84
8	<b>11h</b>	−0.064	−0.51	0.446	2.86	0.14	−0.204	2.82
9	<b>11j</b>	−0.114	−0.18	0.066	2.74	−0.07	−0.044	2.7
10	<b>1</b>	−0.167	−0.03	−0.137	2.82	−0.24	0.073	2.45
11	<b>11k<sup>a</sup></b>	−0.185	0.05	−0.235	2.77	0.04	−0.225	2.73
12	<b>11l</b>	−0.196	−0.57	0.374	2.82	−0.4	0.204	2.63
13	<b>10m<sup>a</sup></b>	−0.199	−0.12	−0.079	2.72	−0.24	0.041	2.39
14	<b>11a</b>	−0.233	−0.06	−0.173	1.9	−0.11	−0.123	2.54
15	<b>11i<sup>a</sup></b>	−0.274	−0.66	0.386	2.35	−0.45	0.176	2.75
16	<b>14c</b>	−0.281	0.61	−0.891	2.51	0.51	−0.791	2.5
17	<b>11d</b>	−0.36	−0.49	0.13	2.54	−0.3	−0.06	2.8
18	<b>13f<sup>a</sup></b>	−0.387	−1.19	0.803	2.74	0.01	−0.397	2.7
19	<b>10i</b>	−0.406	−0.48	0.074	2.81	−0.81	0.404	2.37
20	<b>10l<sup>a</sup></b>	−0.431	−0.36	−0.071	2.69	−0.24	−0.191	2.36
21	<b>13a</b>	−0.431	−0.73	0.299	1.79	−0.32	−0.111	2.22
22	<b>11f</b>	−0.464	−0.54	0.076	2.22	−0.55	0.086	2.79
23	<b>10f<sup>a</sup></b>	−0.496	−0.53	0.034	2.49	−0.48	−0.016	2.42
24	<b>10d</b>	−0.526	−0.31	−0.216	2.24	−0.19	−0.336	1.82
25	<b>13b</b>	−0.526	−0.90	0.374	2.25	−1.14	0.614	2.65
26	<b>11b</b>	−0.631	−0.60	−0.031	2.23	−0.8	0.169	2.78
27	<b>11c<sup>a</sup></b>	−0.678	−0.25	−0.428	2.85	−0.07	−0.608	2.64
28	<b>10j</b>	−0.882	−0.91	0.028	2.79	−0.89	0.008	2.35
29	<b>13d</b>	−0.885	−0.25	−0.635	2.76	0.09	−0.975	2.75
30	<b>10h</b>	−0.991	−0.66	−0.331	2.18	−0.94	−0.051	2.51
31	<b>13e<sup>a</sup></b>	−1.201	−0.90	−0.301	2.23	−1.05	−0.151	2.61
32	<b>14a</b>	−1.301	−0.78	−0.521	2.72	−1.14	−0.161	2.18

<sup>a</sup> Compounds in test set

acids such as VAL 238, CYS 241, ALA 250, LYS 254, LEU 255, LYS 352, and THR 353 are involved in the interaction of all compounds. As defined in constraints, the interaction of standard compound colchicine with the residues of tubulin involved hydrogen bonding with side chain atom S of CYS 241. Similarly, out of three C=O groups, two C=O groups in all compounds except **19** and **32** showed hydrogen binding with SH of CYS 241 and NH of ALA 250 (Fig. 7). Some compounds also showed the hydrogen bonding with O atoms of THR 179, VAL 238,

and LYS 352. 6. It was also found that amino acid residues formed the most of the hydrogen bonding with benzoyl urea chain.

CPHs ADDHR.11 and ADDHR.245 were also correlated with compounds docked at colchicine-binding site of  $\beta$ -tubulin and it was found that C=O group, hydrogen bond acceptor (A1) from CPH ADDHR.11 showed hydrogen binding with SH of CYS 241 (Fig. 8). Hydrogen bond acceptor (A2) vector feature from CPH ADDHR.245 not showed any hydrogen bonding, whereas C=O group near to

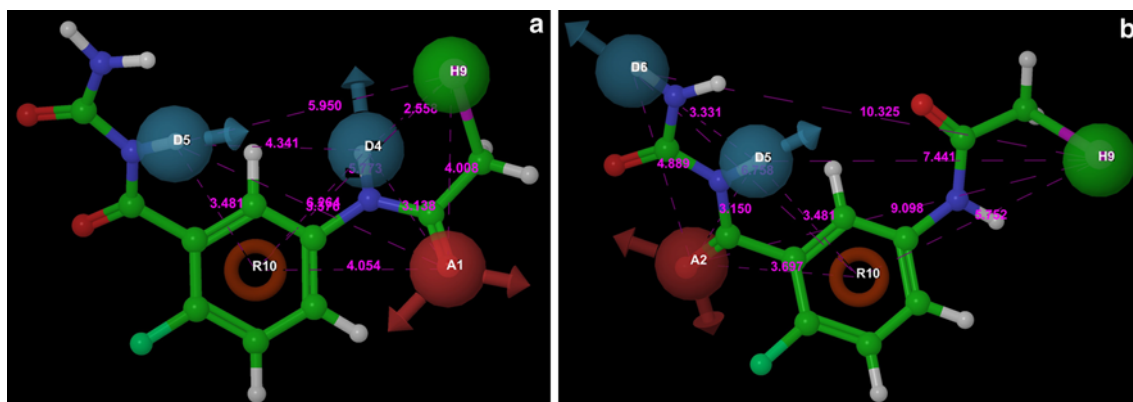


**Fig. 4** Distance between pharmacophoric sites in CPHs: **a** ADDHR.11 and **b** ADDHR.245. All distances are in Å unit

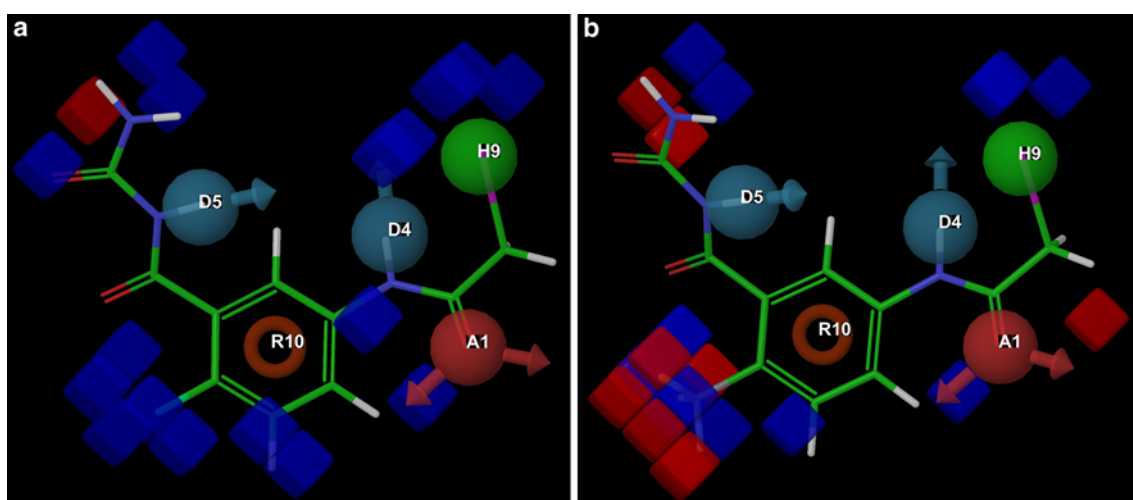


**Fig. 5** Pictorial representation of the cubes generated using the QSAR model developed using CPH ADDHR.11 for **a** most active compound **31** and **b** least active compound **30** in the training set. Blue

*cubes* indicate favorable regions, while *red cubes* indicate unfavorable region for the activity (Color figure online)

hydrogen bond donor (D5) vector feature showed hydrogen bonding with NH of ALA 250. Thus, hydrogen bond acceptor (A1) feature showed importance for the formation of hydrogen bonding with SH of CYS 241.

## Conclusion

The four 3D-QSAR models were developed using variant CPHs which consist of one acceptor, two donors, one hydrophobic, and one ring vector feature. The correctness and capability of both 3D-QSAR models were validated internally by applying to test set and externally by predicting the activity of compounds having benzoyl urea pharmacophore from literature. The one predictive

3D-QSAR models were selected based on statistical results. These 3D-QSAR models provide insight into the structural requirement of benzoyl urea analogs as tubulin agents for antiproliferative activity. Docking studies were also performed and also correlated with CPHs which indicated that all compounds bind in similar pose at colchicine-binding site of  $\beta$ -tubulin. Hydrogen bond acceptor (A1) vector feature showed the hydrogen bonding with SH of CYS 241 in all compounds suggested the importance of 3D-QSAR model developed using CPH ADDHR.11. Thus, this 3D-QSAR model gives a hypothetical image for designing of new potential compounds. The involvement of benzoyl urea core for the interaction with amino acid in colchicine-binding site of  $\beta$ -tubulin suggests its importance as common core for tubulin-binding agents. In conclusion,

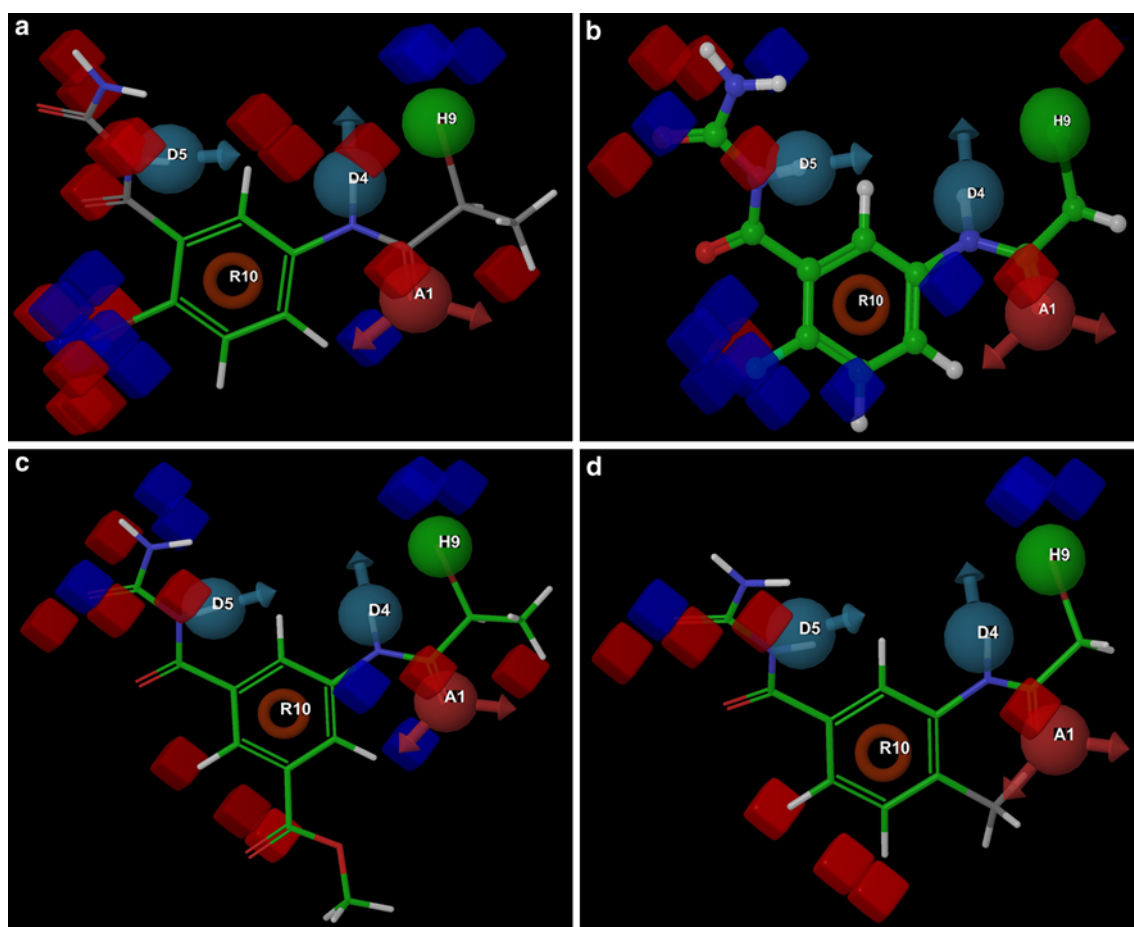


**Fig. 6** Pictorial representation of the cubes generated using the QSAR model developed using CPH ADDHR.11 for **a** compound **8**, **b** compound **26**, **c** compound **9**, and **d** compound **13**. *Blue cubes*

indicate favorable regions, while *red cubes* indicate unfavorable region for the activity (Color figure online)

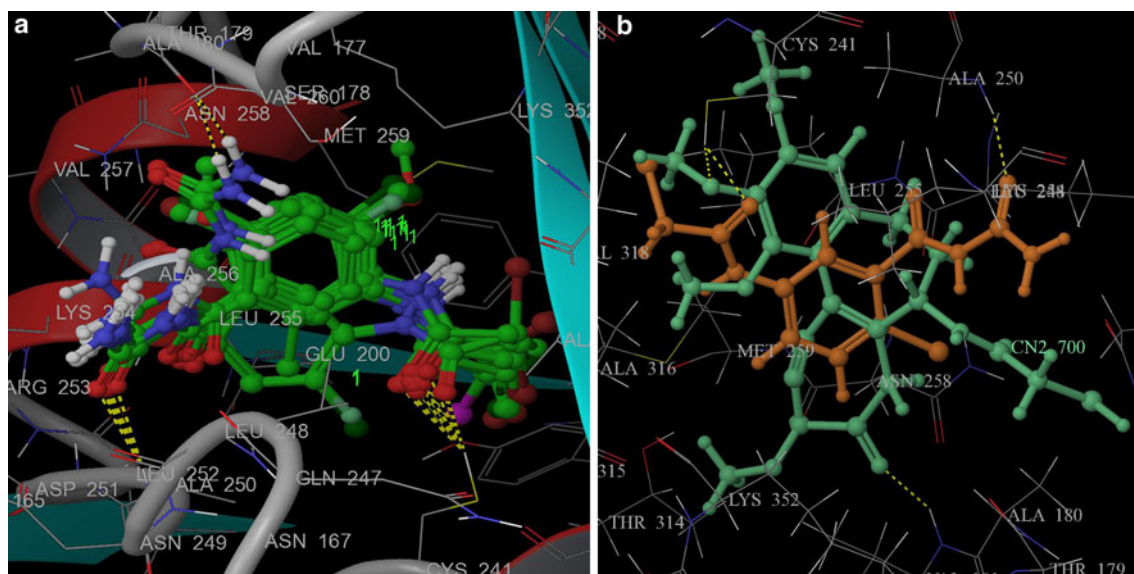
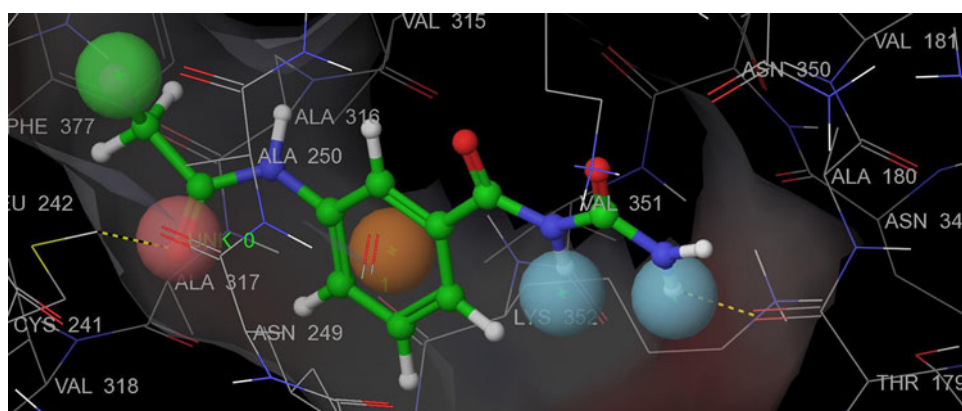


**Fig. 7** Docking of compounds on colchicine-binding site of  $\beta$ -tubulin. **a** Docking pose of all compounds docked and **b** overlap of colchicine and compound **18** at binding site

**Fig. 8** Docking pose of compound **29** at active binding site showing CPH ADDHR.11. Yellow dotted lines show hydrogen binding (Color figure online)



the overall study provides detailed structure and important binding information of benzoyl urea derivatives as tubulin-binding agents for antiproliferative activity.

**Acknowledgments** The authors are thankful to University Grant commission (UGC), New Delhi for financial assistance. The authors are also thankful to the Head, Department of Chemical Technology, Dr. Babasaheb Ambedkar Marathwada University, Aurangabad 431 004 (MS), India for providing all necessary facilities for above work.

## References

- Arora S, Wang XI, Keenan S, Andaya MC, Peng QY, Welsh WJ (2009) Novel microtubule polymerization inhibitor with potent antiproliferative and antitumor activity. *Cancer Res* 69:1910–1915
- Beckers T, Mahboobi S (2003) Natural, semisynthetic and synthetic microtubule inhibitors for cancer therapy. *Drugs Future* 28:767–785
- Dixon SL, Smondryev AM, Knoll EH, Rao SN, Shaw DE, Friesner RA (2006) PHASE: a new engine for pharmacophore perception, 3D QSAR model development, and 3D database screening: 1. Methodology and preliminary result. *J Comput Aided Mol Des* 20:647–671
- Friesner RA, Banks JL, Murphy RB, Halgren TA, Klicic JJ, Mainz DT, Repasky MP, Knoll EH (2004) Glide: a new approach for rapid, accurate docking and scoring. 1 Method and assessment of docking accuracy. *J Med Chem* 47:1739–1749
- Giannakakou P, Sackett D, Fojo T (2000) Tubulin/microtubules: still a promising target for new chemotherapeutic agents. *J Natl Cancer Inst* 92:182–183
- Goodin S, Kane MP, Rubin EH (2004) Epothilones: mechanism of action and biologic activity. *J Clin Oncol* 22:2015–2025
- Hu L, Li Z, Li JN, Qu J, Jiang JD, Boykin DW (2007) 3-(20-Bromopropionylamino)-benzamides as novel S-phase arrest agents. *Bioorg Med Chem Lett* 17:6847–6852
- Hwang KJ, Park KH, Lee CO, Kim BT (2002) Novel benzoylurea derivatives as potential antitumor agents; synthesis, activities and structure–activity relationships. *Arch Pharmacol Res* 25:781–785
- Jeffrey RJ, Denis RP, Mohammed MD, Pearl SH (2007) Targeted anti-mitotic therapies: can we improve on tubulin agents. *Nat Rev Cancer* 7:107–117
- Jiang JD, Denner LY, Ling H, Li JN, Davis A, Wang Y, Li Y, Roboz J, Wang LG, Soler RP, Marcelli M, Bekesi G, Holland JF (2002) Double blockade of cell cycle at G1–S transition and M phase by 3-iodoacetamido benzoyl ethyl ester, a new type of tubulin ligand. *Cancer Res* 62:6080–6088
- Jordan MA, Wilson L (2004) Microtubules as a target for anticancer drugs. *Nat Rev Cancer* 4:253–265
- Jorgensen WL, Maxwell DS, Tirado-Rives J (1996) Development and testing of the OPLS all-atom force field on conformational energetics of organic liquids. *J Am Chem Soc* 118:11225–11236
- Kavallaris M (2010) Microtubules and resistance to tubulin binding agents. *Nat Rev Cancer* 10:1–11
- Kingston DG (2009) Tubulin-interactive natural products as anticancer agents. *J Nat Prod* 72:507–515
- Kiselyov A, Konstantin VB, Sergey ET, Nikolay S, Alexandre VI (2007) Recent progress in discovery and development of antimetabolic agents. *Anti-Cancer Agents Med Chem* 7:189–208
- Li Q, Sham HL (2002) Discovery and development of antimetabolic agents that inhibit tubulin polymerization for the treatment of cancer. *Expert Opin Ther Pat* 12:1663–1702
- Li JN, Song DQ, Lin YH, Hu QY, Yin L, Bekesi G, Holland JF, Jiang JD (2003) Inhibition of microtubule polymerization by 3-bromopropionylamino benzoylurea (JIMB01), a new cancericidal tubulin ligand. *Biochem Pharmacol* 65:1691–1699
- Ling YH, Liebes L, Ng B, Buckley M, Elliott PJ, Adama J, Jiang JD, Muggia FM, Perez-Soler R (2002) PS-341, a novel proteasome inhibitor, induces Bcl-2 phosphorylation and cleavage in association with G2-M phase arrest and apoptosis. *Mol Cancer Ther* 1:841–849
- Ling YH, Liebes L, Jiang JD, Holland JF, Elliott PJ, Adama JF, Muggia M, Perez-Soler R (2003) Mechanisms of proteasome inhibitor PS-341-induced G2-M-phase arrest and apoptosis in human non-small cell lung cancer cell lines. *Clin Cancer Res* 9:1145–1154
- Lokwani D, Shah R, Mokale S, Shastry P, Shinde D (2012) Development of energetic pharmacophore for the designing of 1,2,3,4-tetrahydropyrimidine derivatives as selective cyclooxygenase-2 inhibitors. *J Comput Aided Mol Des* 26:267–277
- Mokale SN, Lokwani D, Shinde DB (2012) Synthesis, biological activity and docking study of imidazol-5-one as novel non-nucleoside HIV-1 reverse transcriptase inhibitors. *Bioorg Med Chem* 20:3119–3127
- Pellegrini F, Budman DR (2005) Review: tubulin function, action of antitubulin drugs and new drug development. *Cancer Invest* 23:264–273
- Pettit GR, Singh SB, Hamel E, Lin CM, Alberts DS, Garcia-Kendall D (1989) Isolation and structure of the strong cell growth and tubulin inhibitor combretastatin A-4. *Experientia* 45:209–211
- Schiff PB, Horwitz SB (1980) Taxol stabilizes microtubules in mouse fibroblast cells. *Proc Natl Acad Sci USA* 77:1561–1565



- Song DQ, Wang Y, Wu L, Yang ZP, Wang YM, Gao LM, Li Y, Qu JR, Wang YH, Li YH, Du NN, Han YX, Zhang ZP, Jiang JD (2008) Benzoylurea derivatives as a novel class of antimitotic agents: synthesis, anticancer activity, and structure–activity relationships. *J Med Chem* 51:3094–3103
- Song DQ, Du N, Wang YM, He WY, Jiang EZ, Cheng SX, Wang YX, Li YH, Wang YP, Li X, Jiang JD (2009a) Synthesis and activity evaluation of phenylurea derivatives as potent antitumor agents. *Bioorg Med Chem* 17:3873–3878
- Song DQ, Wang YM, Du NN, He WY, Chen KL, Wang GF, Yang P, Wu LZ, Zhang XB, Jiang JD (2009b) Synthesis and activity evaluation of benzoylurea derivatives as potential antiproliferative agents. *Bioorg Med Chem Lett* 19:755–758
- Sridhare M, Macapinlac MJ, Goel S, Verdier-Pinard D, Fojo T, Rothenberg M, Colevas D (2004) The clinical development of new mitotic inhibitors that stabilize the microtubule. *Anticancer Drugs* 15:553–558
- Verhey KJ, Gaertig J (2007) The tubulin code. *Cell Cycle* 6:2152–2160
- Wani MC, Taylor HL, Wall ME, Coggon P, McPhail AT (1971) Plant antitumor agents, VI. Isolation and structure of taxol, a novel antileukemic and antitumor agent from *Taxus brevifolia*. *J Am Chem Soc* 93:2325–2327
- Watts KS, Dalal P, Murphy RB, Sherman WR, Friesner A, Shelley JC (2010) ConfGen: a conformational search method for efficient generation of bioactive conformers. *J Chem Inf Model* 50:534–546
- Yoshimatsu K, Yamaguchi A, Yoshino H, Koyanagi N, Kitoh K (1997) Mechanism of action of E7010, an orally active sulfonamide antitumor agent: inhibition of mitosis by binding to the colchicine site of tubulin. *Cancer Res* 57:3208–3213